Electromagnetic three-dimensional reconstruction of targets from free space experimental data

J.-M. Geffrin,[a] P. C. Chaumet, C. Eyraud,[b] K. Belkebir, and P. Sabouroux
Aix-Marseille Université, Ecole Centrale Marseille, and CNRS, Institut Fresnel, Domaine Universitaire de St Jérôme, 13013 Marseille, France

(Received 21 December 2007; accepted 16 April 2008; published online 15 May 2008)

This paper deals with the problem of reconstructing the relative permittivity of three-dimensional targets using experimental scattered fields. The fields concerned were measured in an anechoic chamber on the surface of a sphere surrounding the target. The inverse scattering problem is reformulated as an optimization problem that is iteratively solved thanks to a conjugate gradient method and by using the coupled dipoles method as a forward problem solver. The measurement technique and the inversion procedure are briefly described with the inversion results. This work demonstrates the reliability of the experiments and the efficiency of the proposed inverse scattering scheme. © *2008 American Institute of Physics*. [DOI: 10.1063/1.2924303]

Inverse scattering problems concern a variety of applications such as medical imaging, nondestructive testing, and subsurface probing, in which the properties of unknown targets are determined through their response to outside stimuli. Unlike direct problems, where the aim is to model the interaction of waves with material structures, inverse problems are often ill posed and generally nonlinear. Consequently, it was decided to validate algorithms that solve inverse scattering problems using real data. Over the last few years, we have devoted considerable time and effort to construct an experimental database for inversion purposes. Two special sections published in the Inverse Problems journal[1,2] were dedicated to the reconstruction of homogeneous and inhomogeneous two-dimensional targets from scattered fields measured in our anechoic chamber. The experimental setup used to measure the electromagnetic fields is described in Ref. 3 and the two sets of data, known as the Fresnel Database, are freely available on the IoP website or directly on the Fresnel website. Since the creation of the databases, considerable effort has been made in order to optimize the experimental setup protocol and its control in the case of full vectorial three-dimensional problems, for which few such experimental validations have been done. This study, therefore, presents blind reconstructions of three-dimensional targets from measured scattered fields.

One key issue when dealing with inverse scattering problems is to ensure that the scattered field contains enough information from the target. The relevant quantity of information is, in fact, difficult to determine since it depends on the target under test as well as on the measurement configuration. Nevertheless, we aim to fill the Ewald sphere as much as possible within a time limit of 24 h. Many measurements are therefore needed, i.e., a large number of incidence angles, receiver positions, and/or frequencies. Another solution to render inversion possible is to use as much *a priori* information as possible, such as some knowledge of the symmetry of the studied configuration.[4]

Moreover, to obtain acceptable spatial resolution in all directions, the source and receiver should preferably be moved all around the target. In our anechoic chamber, Fig. 1(a), we were able to make measurements almost everywhere on the surface of the 4 m diameter sphere centered on the target by using a combination of three main mechanical movement devices; a circular vertical arch, the rotation of the receiver around the target, and the rotation of the target itself. Hence, filling the Ewald sphere is mainly limited by the physical movement around the arch and by the measurement period.

A referential frame applied to the target, as in Fig. 1(b), provides 81 source positions, evenly spaced along 9 parallels and 9 meridians, as depicted in Fig. 2(a), and 27 receiver positions [Fig. 2(b)]. This means that 2187 measurements can be made almost completely around the target for each polarization. In fact, our experimental setup limits receiver movements to an azimuthal rotation of 260° ($\phi_r=90°$) and the placing of an antenna no closer to the source meridian than 50°. Furthermore, some other measurements are also excluded due to the saturation of the network analyzer re-

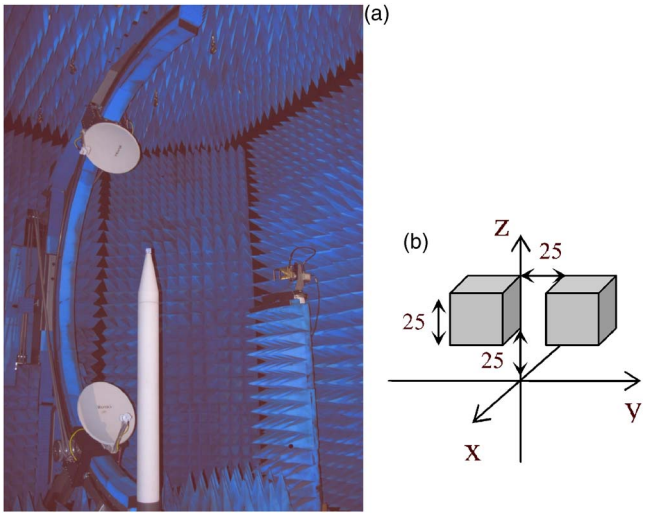

FIG. 1. (Color online) (a) Experimental setup with two transmitting parabola and a ridged horn antenna as receiver. (b) Scattering target: two 25 mm polyethylene cubes ($\varepsilon=2.35$) spaced by 25 mm.

[a]Electronic mail: jean-michel.geffrin@fresnel.fr.
[b]Present address: Laboratoire de Planétologie de Grenoble, Université J. Fourier, CNRS, 38041 Grenoble, France.

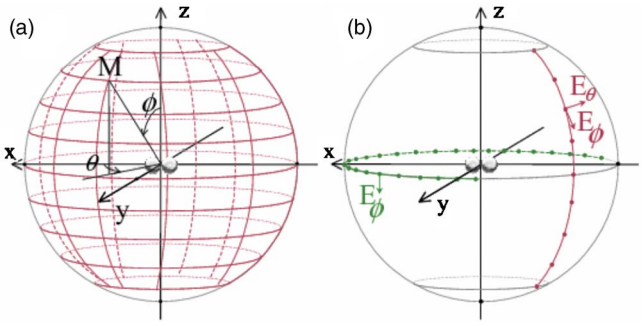

FIG. 2. (Color online) (a) Source positions ϕ_s from 30° to 150° step 15° and θ_s from 20° to 340° step 40°. (b) Receiver positions θ_r from 0° to 350° step 10° but with mechanical and saturation exclusions.

ceiver, which occurs when the receiving antenna is in front of the parabola.

All the measurements that are presented here were obtained with the anechoic chamber at the Institut Fresnel, using a HP8510 network analyzer, external mixers, two parabolic antennas (Hyptra NE5256) as sources, and a ridged horn (ARA DRG 118) as a receiving antenna. The use of two parabolas connected to a switching device which alternately selects them allows a reduction in the measurement time by a factor of almost two. Due to the parabola bandwidth, the operating frequency is varied from 3 to 8 GHz with a step of 0.25 GHz to respect our time limitation (see Ref. 3 for more details concerning the description of the equipment). Both $\phi\phi$ and $\theta\phi$ polarizations are measured using a mechanical rotation of the parabola. As the targets under test measure only a few cubic wavelengths, they are very low scatterers especially at the lowest operating frequencies, and the accuracy of the measurements becomes critical for such scattering measurements.[5]

In order to be able to perform quantitative inversions (i.e., retrieval of the permittivity distribution), measurement calibration was required. After different trials, the calibration procedure that we decided to apply is based on the measurement of the scattered field for a reference target measured only on the (xOy) plane and the $\theta\theta$ polarization case. A single, complex coefficient, computed for each frequency, is then deduced from the comparison of the measured scattered field and the simulated one. In the present case, a 70 mm diameter metallic sphere was used as a reference target and the simulated field was derived from the Mie theory. A plane wave illumination is considered in the simulations, which is consistent with the use of a parabolic antenna as source. In the case of long measurement periods, and weak scatterers, drift errors are no longer negligible. We therefore designed an original drift compensation solution, based on the minimization of the spectral bandwidth of the scattered field, and used it to remove this specific noise from the measured scattered field.[6] As a result, we were able to use the calibrated scattered fields that we obtained to perform blind reconstruction of dielectric targets.

As far as the inverse scattering problem is concerned, it is iteratively solved. It is assumed that the target under test is confined to a bounded box Ω where the permittivity (or the refractive index) distribution varies and differs from that of the background. Then, starting from an initial guess, based on the back-propagation technique,[7] the permittivity is gradually adjusted. The adjustment of the permittivity distribution ε of the sample is deduced by minimizing the cost functional of the following form[7,8]

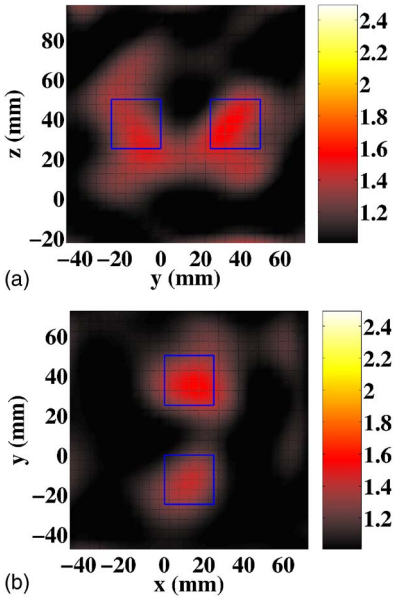

FIG. 3. (Color online) Cross sections of the permittivity profile obtained after inversion at 3 GHz ($\lambda/4=25$ mm). (a) Relative permittivity in plane (y,z) at $x=12.5$ mm. (b) Relative permittivity in the plane (x,y) at $z=37.5$ mm.

$$\mathcal{F}(\varepsilon) = \sum \|\mathbf{F}^{\mathrm{sca}}(\theta_s, \phi_s, \theta_r) - \mathbf{E}^{\mathrm{sca}}(\theta_s, \phi_s, \theta_r; \varepsilon)\|^2, \tag{1}$$

where $\mathbf{F}^{\mathrm{sca}}$ is the "experimental" data and $\mathbf{E}^{\mathrm{sca}}$ is the simulated field radiated with the best available estimated permittivity ε. Notice that the sum is calculated using all the receiver and source positions. The minimization of the cost functional of Eq. (1) is achieved numerically using a conjugate gradient algorithm.

For each iteration step, the forward scattering problem is solved in order to evaluate $\mathbf{E}^{\mathrm{sca}}$. As a forward solver, we use the coupled dipole method (CDM), which is equivalent to the moment method.[9,10] The basic ideas underlying the CDM is to represent the object under study by a cubic array of N polarizable subunits of side d. If the subunits are small compared to the wavelength inside the object $(d \ll \lambda/\sqrt{\varepsilon})$, the local field at each subunit can be considered as uniform and can be expressed as

$$\mathbf{E}^{\mathrm{loc}}(\mathbf{r}_i) = \mathbf{E}^{\mathrm{inc}}(\mathbf{r}_i) + \sum_{j=1, j\neq i}^{N} \mathbf{T}(\mathbf{r}_i, \mathbf{r}_j)\alpha(\mathbf{r}_j)\mathbf{E}^{\mathrm{loc}}(\mathbf{r}_j), \tag{2}$$

where $\mathbf{r}_i$ is the position of the ith subunit, $\mathbf{E}^{\mathrm{inc}}(\mathbf{r}_i)$ the incident field at the position $\mathbf{r}_i$ (i.e., the field at the position $\mathbf{r}_i$ in the absence of the object), and $\mathbf{T}$ the linear response to a dipole in free space. $\alpha(\mathbf{r}_j)$ is the polarizability of the subunit j and is related to the Clausius Mossotti relation.[9] Once the local field is obtained at each subunit, by solving the linear system represented by Eq. (2), the field scattered by the object at an arbitrary position $\mathbf{r}$ is

$$\mathbf{E}^{\mathrm{sca}}(\mathbf{r}) = \sum_{i=1}^{N} \mathbf{T}(\mathbf{r}, \mathbf{r}_i)\alpha(\mathbf{r}_i)\mathbf{E}^{\mathrm{loc}}(\mathbf{r}_i). \tag{3}$$

Thus, by applying the experimental procedure and the inverse scattering scheme previously described, we were able to reconstruct the object depicted in Fig. 1(b). The recon-

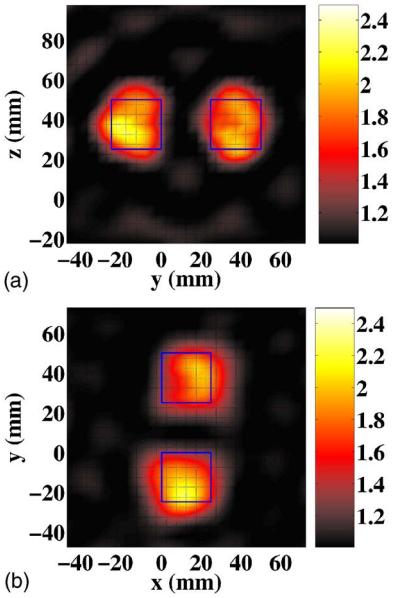

FIG. 4. (Color online) As in Fig. 3 but at 6 GHz ($\lambda/2=25$ mm).

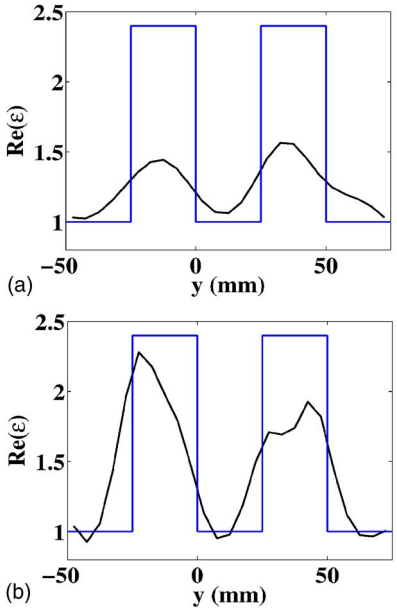

FIG. 5. (Color online) Profile of the permittivity vs y at $x=12.5$ mm and $z=37.5$ mm obtained after inversion in black line. The actual profile is plotted in blue line. (a) 3 GHz. (b) 6 GHz.

structions obtained for these two dielectric cubes are presented in Figs. 3–5 for the two operating frequencies 3 and 6 GHz. With the operating frequency of 3 GHz, the cubes and the space between them are smaller than half a wavelength ($\lambda/4$) and we can nevertheless observe an approximate localization of the two cubes. However, the two cubes are not clearly separated nor are their dielectric characteristics accurately estimated, as illustrated by the y axis cross sections plotted in Figs. 3 and 5 comparing the reconstructed profiles and the actual ones. The spacing lattice used here is $d=5$ mm and the investigated volume Ω is a cube with the dimensions $125\times125\times125$ mm^3.

For the higher frequency, i.e., 6 GHz, the results of the reconstructions are presented in Figs. 4 and 5(b). One can observe that both the shape and the constitutive material of the two cubes are correctly retrieved, and, as expected, the resolution is improved when the operating frequency is increased.

In this letter, we tackled the problem of the characterization of three-dimensional targets from measured scattered fields. Special care was taken in the experiments to reduce the different kinds of noise, in particular to compensate for drift errors. Using this data, blind reconstruction was performed and brought about satisfactory results insomuch that the shape and permittivity of the unknown target were correctly reconstructed. Thus, we have been able to demonstrate the reliability of the measurements, as well as the robustness against the presence of noise in the data of the inverse scattering algorithm. Future developments will consider more complex targets and different configurations, such as the ones encountered when probing subsoil.

[1] K. Belkebir and M. Saillard, Inverse Probl. **17**, 1565 (2001).
[2] K. Belkebir and M. Saillard, Inverse Probl. **17**, S1 (2005).
[3] J.-M. Geffrin, P. Sabouroux, and C. Eyraud, Inverse Probl. **21**, S117 (2005).
[4] J. D. Zaeytijd, A. Franchois, C. Eyraud, and J.-M. Geffrin, IEEE Trans. Antennas Propag. **55**, 3279 (2006).
[5] C. Eyraud, Ph.D. thesis, Univ. Provence—Aix Marseille I, 2006.
[6] C. Eyraud, J.-M. Geffrin, A. Litman, P. Sabouroux, and H. Giovannini, Appl. Phys. Lett. **89**, 244104 (2006).
[7] K. Belkebir, P. C. Chaumet, and A. Sentenac, J. Opt. Soc. Am. A **22**, 1889 (2005).
[8] K. Belkebir, P. C. Chaumet, and A. Sentenac, J. Opt. Soc. Am. A **23**, 586 (2006).
[9] P. C. Chaumet, A. Sentenac, and A. Rahmani, Phys. Rev. E **70**, 036606 (2004).
[10] A. Rahmani, P. C. Chaumet, and G. W. Bryant, Astrophys. J. **607**, 873 (2004).